Düzce University
Journal of Science & Technology

Research Article

Analysis And Improvement of Poor Bearing Capacity Soils in Düzce Province by Jet grouting Method

Ali ATEŞ [a], Burak YEŞİL [b,*], Şükrü ÇİMEN [c], Serdal ALEMDAR [d]

[a] *Faculty of Engineering, Civil Engineering Department, Bolu Abant İzzet Baysal University, Bolu, TURKEY, (ORCID:0000-0001-6297-85-71)*
[b] *Construction Technology, Düzce Vocational School, Düzce University, Düzce, TURKEY (ORCID: 0000-0001-5320-9359)*
[c,d] *Ministry of Environment, Urbanisation and Climate Change, Düzce Provincial Directorate, Branch Directorate Responsible for Building Inspection and Building Materials, Düzce, TURKEY*
** Corresponding author's e-mail address: burakyesil@duzce.edu.tr*
DOI: 10.29130/dubited.1548995

ABSTRACT

Turkey is situated in an earthquake-prone zone, and due to its geographic location, Düzce is among the most hazardous regions in the country and the world. The seismic risk in Düzce province is significantly influenced by the North Anatolian Fault (NAF), which is characterized by an active tectonic structure. This area has experienced earthquakes of varying magnitudes both before and after the instrumental recording period. Especially, two significant earthquakes occurred in 1999: on August 17, an earthquake with a moment magnitude of Mw = 7.4 struck the Adapazarı-İzmit region. Shortly after, on November 12, 1999, another earthquake with a moment magnitude of M_w=7.1 hit Düzce area at approximately 18:57, lasting for about 30 seconds. During the August 17 earthquake, the eastern section of the Düzce fault, measuring 43 km, was activated. The November 12 earthquake is considered to have been triggered by the previously unbroken eastern section of the Düzce fault as a result of the initial faulting. In the city center, the soil composition mainly consists of fine gravel and sandy gravel in certain areas. Previous earthquakes have resulted in structural damages primarily due to bearing capacity issues, and liquefaction phenomena have also been observed in some locations. In this study, the soil beneath a planned three-story building in Düzce, an area identified having a liquefaction risk, was improved using the jet grout method.

Keywords: *Bearing capacity, Jet groud, Ground improvement, Geotechnical*

Düzce İlinde, Taşma Gücü Zayıf Zeminlerin Jet grout Yöntemi ile Analizi ve İyileştirilmesi

ÖZ

Türkiye bir deprem kuşağı üzerinde bulunmaktadır. Ülkemizin üzerinde bulunduğu kuşak itibari, Düzce ile Dünyanın ve ülkemizin en riskli bir bölgesinde bulunmaktadır. Düzce ilinin depremsellik riski Kuzey Anadolu Fayı (KAF) etkisinde bulunmaktadır. Bu bölge aktif bir tektonik yapıya sahiptir. Aletsel dönem öncesinde ve sonrasında değişik zamanlarda farklı büyüklükte depremlere maruz kalmıştır. Son dönemde 1999 yılında iki farklı deprem meydana gelmiştir; 17 Ağustos 1999 tarihinde Adapazarı İzmit bölgesinde deprem moment büyüklüğü M_w=7,4 büyüklüğünde bir deprem meydana gelmiştir. 12 Kasım 1999 tarihinde akşam saatlerinde yaklaşık 18.57'de Düzce'de deprem moment büyüklüğü M_w=7,1 olan bir deprem kaydedilmiş ve 30 s sürmüştür. 17 Ağustos 1999 depreminde Düzce fayın 43 km uzunluğundaki doğu bölümü kırılmıştır. 12 Kasım 1999 depremi ise, 17 Ağustos 1999'daki faylanmanın Düzce fayının kırılmayan doğu bölümünün tetiklemesi sonucu meydana geldiği düşünülmektedir. Şehir içi yer yer ince çakıl ve kumlu çakıl şeklinde bir semin formasyonuna

Received: 13/09/2024, Revised: 28/10/2024, Accepted: 31/10/2024

sahiptir. Önceki depremlerde daha çok taşıma gücüne bağlı olarak yapı hasarları meydana gelmişse de yer yer sıvılaşma olgularına da rastlanılmıştır. Bu çalışmada Düzce ilinde sıvılaşma riski olan alanda yapılması düşünülen üç katlı yapının üzerine oturacağı zemin iyileştirme yöntemlerinden Jet grout yöntemi kullanılarak iyileştirilmiştir.

Anahtar Kelimeler: *Taşıma gücü, Jet groud, Zemin İyileştirme, Geoteknik*

I. INTRODUCTION

Jet grouting is a versatile and widely adopted soil improvement method. It involves injecting a high-pressure grout mixture into the ground to form soil-cement columns, which improve the mechanical properties of the soil. The technique is particularly effective in weak and soft soils, enhancing load-bearing capacity and mitigating settlement issues. In recent years, several studies have focused on optimizing jet grout applications through numerical modeling, experimental research, and the integration of advanced computational methods such as artificial neural networks (ANNs).

The impact of jet grout columns on soil settlement have been explored in many studies. A study is conducted at Sakarya University used Plaxis 2D and 3D software to analyze the effects of jet grout columns with varying geometrical parameters on soil settlement. It was concluded that jet grout columns significantly reduced settlement, with reductions of up to 22% depending on the column length, spacing, and diameter. It was also noted that increasing the diameter could lead to group effects, which might reduce efficiency.

A similar study by Wang et al. examined the lateral displacement caused by jet grouting in clayey soils and found that the method substantially improved soil stability, particularly in reducing horizontal displacement [1]. Furthermore, Shen et al. highlighted the potential of jet grouting in enhancing bearing capacity and minimizing settlement, especially in liquefaction-prone soils [2].

Jet grouting has also proven the effective in reducing liquefaction potential in earthquake-prone areas. Shen et al. showed that jet grout columns significantly improved the stability of liquefiable soils by increasing their bearing capacity and reducing pore water pressure. The ability of jet grout columns to enhance soil cohesion and mitigate liquefaction risks makes this method highly valuable for projects in seismic regions [2].

Jet grouting has also been extensively studied for its applications in organic and peat soils, which are characterized by low shear strength and high compressibility. Yalçın et al. investigated the use of jet grout columns in undisturbed peat soils and found that the bearing capacity increased by four times for square foundations and 4.5 times for strip foundations [3].

Wong et al. similarly evaluated jet grout applications in soft marine clays, demonstrating that large-diameter columns effectively improved soil stability. Their work underlines the importance of column diameter and length optimization for achieving maximum ground improvement [4].
In a related study, Güllü utilized genetic programming to predict the rheological properties of jet grout mixtures, improving the overall efficiency and performance of jet grout applications. The integration of ANN and other machine learning techniques presents a valuable opportunity for optimizing jet grouting in various soil conditions [5].

One of the critical challenges in jet grouting applications is predicting soil displacement under various loading conditions. In a study carried out in Konya, Turkey, ANN models were used to predict settlement and displacements in a site where 3,351 jet grout columns were installed. The models used input parameters such as grout column length, diameter, and applied loads, achieving highly accurate displacement predictions [6].

Jet grouting is widely applied in a range of geotechnical projects, including foundation strengthening, tunnel construction, and slope stabilization. Lenard et al. emphasized the importance of optimizing column geometries and grout compositions to achieve the desired performance in various soil conditions [7].

Recent studies have also highlighted the need for continued research into jet grouting optimization, particularly through the use of advanced numerical modeling techniques. Vu and Le discussed the effectiveness of large soil-cement columns in improving soil characteristics and emphasized the need for further studies on grout distribution and column arrangement in challenging soil types [8].

Turkey is situated in the Alpine-Himalayan earthquake zone, leading to frequent seismic activity throughout the country. Both historical and instrumental records indicate that Turkey has experienced various earthquakes, resulting in significant loss of life and property. Given the persistent earthquake risk, it is imperative to construct earthquake-resistant structures to coexist with this natural threat. Düzce province lies along the North Anatolian Fault (NAF) system, where losses in bearing capacity are commonly observed during earthquakes. Past seismic events have revealed structural failures primarily attributed to bearing capacity issues in the superstructure.

Soil-related failures, including those caused by liquefaction, have also impacted infrastructure. Bearing capacity failures typically occur in soft and weak soils. In sandy and alluvial soils, the presence of groundwater can lead to liquefaction under the shear forces generated by an earthquake. Areas with liquefaction potential often experience significant loss of bearing capacity, resulting in damage to structures situated on these compromised soils.

Düzce province features alluvial and fine-grained sandy gravel soils, which pose challenges for construction. Therefore, any structures built on weak soils or those with a risk of liquefaction must undergo ground improvement before construction [9]. In this context, the soil beneath a planned approximately 1,000 m² building with a basement, ground floor, and three additional stories set to be constructed by the Düzce Provincial Directorate of the Ministry of Family and Social Policies on a 1,918.84 m² parcel (No. 535) in Kiremitocağı Neighborhood, Central District has been reinforced to enhance its earthquake resistance.

Table 1. *Symblos and explanations*

Symbol	Explanation	Symbol	Explanation
a_{max}	Maximum horizontal ground acceleration	A_{JG}	Area Relocation Rate
σ_{vo}	Total vertical stress (kN/m^2)	D_a	Average diameter
$\sigma_{vo'}$	Effective vertical stress (kN/m^2),	K_o	Coefficient of ground pressure at rest
τ_{ave}	Average cyclic stress resistance (kN/m^2)	K_s	Soil pressure coefficient
r_d	Strain reduction coefficient	$P_{ul(grup)}$	Load-bearing capacity of the jet grout column group
$\sigma_{V'}$	Effective vertical stress with unit (kPa)	Q_b	Terminal unit carrying capacity at depth H
δ	Friction angle between ground and column	$Q_{12(ort)}$	Average lateral friction value at depth h_2
α	Reduction factor for adhesion	$Q_{11(ort)}$	Average lateral friction value at depth h_1
c_u	Sliding resistance undrainage	$(N_1)_{60}$	Corrected hit count
ζ	Reduction factor for ultimate load capacity	$(N_{1.60})_{cs}$	Number of SPT strokes corrected for fines.
ν	Poisson's ratio	c	Cohesion
γ	Unit weight of the soil.	f	Internal friction angle

Table 1 (cont). *Symblos and explanations*

ρ	Density based on longitudinal ground shear wave velocity given by Telford 1976	**g**	Gravitational acceleration
A_b	Column base area	G_{JG}	Shear Modulus (MPa)
N_{q*}	Load-bearing capacity coefficient for deep foundations	**R**	The diameter of the column to be constructed under the foundation after the excavation of the foundation.
σ_{vo}	Vertical soil pressure	**z**	Depth (m)
β	Reduction factor	C_N	Load correction factor
CRR	Cyclic resistance ratio	C_R	Drill rod length coefficient
CSR	Cyclic stress ratio	C_S	Sheath coefficient
B	Block width	C_B	Drilling diameter coefficient
L	Block length	C_E	Energy correction coefficient
$L=B_x$	Foundation long side	G_r	Ratio to shear modulus
$B=B_y$	Foundation short side	G_s	Maximum shear modulus of soil
Bk_x, Bk_y	Distance to the nearest column's foundation corner	**H**	Layer depth (m)
D_f	Foundation excavation	**I**	Structure importance coefficient
FC	Fine grain ratio of the soil	**F**	A correction factor depending on the ground type
M_v	Volumetric compression coefficient	h_1	Thickness of the soft layer at which negative surface friction can be produced
M_w	Earthquake moment magnitude	h_2	The carrier layer in which the column is well embedded
P_u	Colony bearing capacity	a_r	Area displacement rate
P_{base}	Colony endpoint bearing capacity	**n**	Number of rows in the horizontal direction
P_{lat}	Column lateral bearing capacity	**m**	Number of rows in the vertical direction
$P_{ul(column)}$	The load-bearing capacity of a single jet grout column	**FS**	Factor of safety
S_y, S_x	Distance between columns	**A**	Unit cell area
		V_s	Ground shear wave speed (m/s)

II. MATERIAL AND METHOD

A. STUDY AREA

The site under consideration is a 1,000 m² building comprising a basement, ground floor, and three additional stories. This project is being planned by the Düzce Provincial Directorate of the Ministry of Family and Social Policies on parcel 535, which measures 1,918.84 m², located in the Kiremitocağı Quarter of the Central District in Düzce province (Figure 1). Since this structure is located is soft soil, the soil needs to be improved and is shown in the figure 1. Also the ground water level is high in the area. The mentioned area is under the effect of Duzce fault that is the ability of potential earthquake occurance.

Figure 1. *Jet grout soil improvement study area*

A. 1. Field Studies

The site for a building with a basement, ground floor, and three additional stories, covering approximately 1,000 m², is planned to be constructed by the Düzce Provincial Directorate of the Ministry of Family and Social Policies on a 1,918.84 m² parcel (No. 535) in the Kiremitocağı Quarter of the Central District. This location is situated in an earthquake zone, specifically along the North Anatolian Fault System (NAF). Three borings, each measuring 12.50 m (sk1-sk2-sk3), were conducted on the site. A simplified geological cross-section has been provided based on the land application and drilling studies carried out in the field (Figure 2).

Figure 2. *Land drilling locations*

Some index parameters related to the soil were obtained in the drilling works carried out in the area where soil improvement is considered. According to the revised zoning plan approved on 11.03.2005, it is located in Precautionary Area 2 (PA-2), where construction is not allowed without precautions. Soil group 'D' and local soil class 'Z4', T_A:0,20 sec, T_B:0,90 sec was determined for the parcel. The geological unit in the study area is Qal (alluvial fan) unit (clay, silt sand) of Plio-Quaternary age and soil type is (ML-MH-SM-SC-GM) according to TS 1500 [20] (Table 1).

Table 2. *Simplified Geological Sil Section Values*

SK1			SK-2		SK-3	
Depth (m)	**Soil Type**	**Ground Water Table (m)**	**Depth (m)**	**Soil Type**	**Depth**	**Soil Type**
1,5	CL		1,5	CL	1,5	CL
3	CH		3	CH	3	CH
4,5	CH	4	4,5	CH	4,5	CH
6	CL		6	CL	6	CL
7,5	CL		7,5	CL	7,5	CL
9	SM	9	9	SM	9	SM
10,5	SC		10,5	SC	10,5	SC
12	GM		12	GM	12	SM

B. METHOD

B.1. Criteria for Determination of Liquefaction Potential

The method proposed by Seed and Idriss, known as the "simplified method," is commonly used in liquefaction analyses [10]. Liquefaction calculations can be performed using Standard Penetration Test (SPT) field data obtained from boreholes in the study area. In this method, two basic parameters must be estimated to determine the potential for liquefaction.

The first is the ratio of the dynamic or cyclic stress ratio (CSR), which represents the earthquake energy potential in the soil layers and characterizes the strength of the seismic waves generated by the earthquake. This ratio compares the response of the soil to horizontal shear stress, providing a safety factor that indicates the condition of the soil (Eq. 1).

$$FS = CRR/CSR \quad (1)$$

If the liquefaction safety factor obtained from this equation is less than 1, it indicates a liquefaction hazard at the site. Conversely, if the safety factor is greater than 1, it suggests that the site is not risky for liquefaction.

Also referred to as the simplified approach, the value of the cyclic stress ratio generated by earthquake forces during seismic events can be calculated using Eq. 2 [10].

$$CSR=0,65\ (a_{max}/g)\ (\sigma_v/\sigma'_v)r_d \quad (2)$$

The effective stress reduction coefficient can be determined according to Liao and Whitman [11] as follows (Eq.3, Eq.4);

$$r_d = 1- 0,00765z \qquad z \leq 9.15\ m \quad (3)$$

$$r_d=1.174-0.0267 \qquad 9.15<z\leq 23 \quad (4)$$

This area is seismically active and lies within the North Anatolian Fault system (NAF). Historical and instrumental records confirm that this region experiences significant seismic activity. In previous years, two major earthquakes occurred along the Düzce Fault, with magnitudes of 7.40 and 7.20 on

August 17, 1999, and November 12, 1999, respectively. According to the literature, it is estimated that the fault may rupture along one-third of its length [12].

In the event of an earthquake occurring in the study area, the moment magnitude is expected to be 7.2, with a maximum horizontal ground acceleration expected to reach 0.51 g [13][14]. To assess the liquefaction potential of the study area, the $(N_1)_{60}$ value was derived from the Standard Penetration Test (SPT) data obtained through drilling in the site.

Estimating the cyclic resistance ratio, the corrected SPT blow count can be calculated using the following equation (Eq. 5), which takes into account factors such as cover load, drill rod length, casing, borehole diameter, and energy correction coefficients. In this context, $(N_1)_{60}$ is defined as follows:

$$(N_{1\cdot 60})_{CS}=N_{land}\ CS.C_E.C_N.C_B.C_R \quad (5)$$

The overburden correction factor can be found by Eq. 6 proposed by Liao and Whitman. [11]

$$C_N = \frac{1.7}{0.7+0.01*\sigma_{V'}} \quad (6)$$

It was proposed to correct the SPT numbers according to the fine grain ratio by considering the effect of the fine grain ratio of the soil with the following equation (Eq.7-Eq.11) [15].

$$(N_{1\cdot 60})_{CS} = \alpha+\beta N_{1,60} \quad (7)$$

$$FC \leq \%5 \text{ için } \alpha=0 \text{ ve } \beta=1 \quad (8)$$

$$\%5<FC<\%35 \text{ için } \alpha=\exp\left(1.76-\frac{190}{(FC)^2}\right) \quad (9)$$

$$\beta=\left[0.99+\left(\frac{FC}{1000}\right)^{1.5}\right] \quad (10)$$

$$FC \geq \%35 \text{ için } \alpha=1 \text{ ve } \beta=1,2 \quad (11)$$

For an earthquake with a moment magnitude of $M_w = 7.5$, Seed and Idriss proposed a cyclic resistance ratio (CRR) based on the $(N_1)_{60,CS}$ values, as expressed in Equation (Eq. 12). This equation illustrates the response of soils in relation to their liquefaction behavior [10].

$$CRR=\frac{1}{34-(N_1)_{60,CS}}+\frac{(N_1)_{60,CS}}{135}+\frac{50}{[10(N_1)_{60,CS}+45]^2}-\frac{1}{200} \quad (12)$$

Here, the Idriss correction coefficients given by C_E are 0.75 for a safe ram type for this effective energy development deployment, and 0.75, 0.85, 0.95 and 1.00 for the correction in the length of the rod, depending on the length of the rod, with a temperature correction of 1.0 for the standard bit copy receiver. In addition, according to the literature of A. W. Skempton, it is understood that the borehole diameter correction is also 1.0 [16].

B.2. Bearing Strength of Jet grout Columns

The jet grout method is a ground improvement technique with a wide range of applications, suitable for nearly all types of soil. This technique involves cutting the ground with a high-pressure water or water-air mixture, and then injecting cement grout at high pressure to fill the resulting voids.

Jet grouting technology can be categorized into three types based on the systems used: single-fluid, double-fluid, and triple-fluid. Generally, two different methods are employed to calculate the bearing capacity of existing jet grouting columns. The first method treats the jet grouting column as a distinct structural element, while the second method applies principles similar to those used for pile bearing capacity.

Due to its production method, the jet grout column is blended with the surrounding natural soil through direct contact. Additionally, the cross-section of the jet grout column can be regularized, featuring either a recessed or rough structure. As a result, the interaction between the natural soil and the jet grouting column is typically more effective than that achieved through driving or pre-piling, even in fine or coarse-grained soils.

A jet grouting expert should regard the technique as a form of soil stabilization, and the bearing capacity of jet grouting columns should be considered as group bearing capacity. Consequently, the bearing capacity of a group of jet grouting columns is accepted as block bearing capacity in design calculations. Block bearing capacity can be utilized in two different ways in programming: the primary method focuses on the bearing resistance of the jet-grouted pavement, while the broader method is presented without controlling ground settlements. In this project, it was decided to extend the design according to the first approach.

To determine how effectively the jet grout columns can transfer structural loads to the ground in the field, a thorough calculation is necessary. There are various methods available for these computations. In this study, the two main dimensions and earthquake parameters presented in table 2,3 are analysed.:

Table 3. *Limit values used for column design in granular soils.*

	Long side (m)	**Short side (m)**	**Excavation depth (m)**	**Nearest column distance from the foundation corner (m)**	**Number of columns in the x direction**	**Number of columns in the y direction**	**Column length after excavation (m)**	**Column diameter**	**Distance between columns (m)**	**Groundwater level after excavation (m)**
Larger foundation	36.78	26.79	3.70	0.5	12	9	12	0.8	3.18 and 2.79	0.3
Smaller foundation	16.8	4.8	3.70	0.5	6	2	12	0.8	3.00 and 3.00	0.3

Table 4. *Groundwater and Earthquake Parameters*

Description	**Value**
Unit Weight of Water (kN/M^3)	10
Water Level (m)	0,3
Magnitude of Earthquake	7.2
Short Period and Short Period Design Spectral Acceleration coefficient	0,414

Additional parameters are detailed in the appendix. The summary of the jet grouting results, including 12 columns, totals 120 columns (108+12), and is illustrated in Tables 4 to 6.

Table 5. *Land drilling locations*

Parameters	**Foundation 1**	**Foundation 2**
x coordinate	0	10,15
y coordinate	0	27,10
S_x	3,18 m	3 m

Table 5 (cont). *Land drilling locations*

S_y	2,94 m	3 m
Number of columns (x)	12	6
Number of columns (y)	9	2
Total number of columns	108	12
Bk_x	0,5 m	0,5 m
Bk_y	0,5 m	0,5 m
B_x	36,78 m	16,80 m
B_y	26,79 m	4,80 m

Table 6. *Soil parameters*

Parameters	**Values**
Unit volume weight	18,33 kN/m^3
Internal friction angle	3^o
Cohesion	32 kN/m^2
Adhesion reduction factor	0,45
Modulus of elasticity	552200 kN/m^2
Poisson ratio	0,46
Water saturated unit volume weight	19,00 kN/m^3
Horizontal restitution coefficient	1
Unimproved soil safety stress	81 kN/m^2
Free compressive strength	100 kPa
Factors related to ground conditions	1
SPT N	26
Fine content	%95
Correction factor depending on soil type	1,029

Table 7. *Column Parameters*

Parameters	**Values**
Jet-groud diameter	0,80 m
Unit volume weight	18,33 kN/m^3
Free compressive strength	6 MPa
Material safety factor	2
Reduction factor for jet-groud column end bearing capacity	1

B.3. Jet grout Columns Bearing Strength Methods

If the Jet grout column is considered as a separate structural element in itself, the bearing capacity of the Jet grout column is calculated as the pile bearing capacity as Eq.13 [17].

$$P_u = P_{base} + P_{lat} \quad (13)$$

For cohesionless (sandy) soils, Eq.14;

$$P_u = A_b\, q_b + \Pi D_a \int_{l_1}^{l_2} \gamma z\, K_s tang\delta d_z \quad (14)$$

Eq.15 for cohesive soils;

$$P_u = A_b\, q_b + \Pi D_a \int_{l_1}^{l_2} \alpha\, c_u d_z \quad (15)$$

Cohesionless, i.e. coarse-grained soils;
The end resistance of the arm can be found with Eq.16;

$$q_b = \frac{1+2K_o}{2}\, \sigma_{vo} N_q^* \xi \quad (16)$$

For cohesive soils, i.e. fine-grained soils, Eq. 17;

$$qb = 9c_u \quad (17)$$

Jet grout columns are vibrated with the jet grout column together with the compaction process on the ground. The studies carried out, it is seen that the cross-sectional part of the Jet grout column is wavy and rough and thus does not form a smooth structure. This is since the communication between the natural soil and the jet grout column is much more intense in clay or cohesionless soils compared to driven or pre-piles. (Figure 3-4).

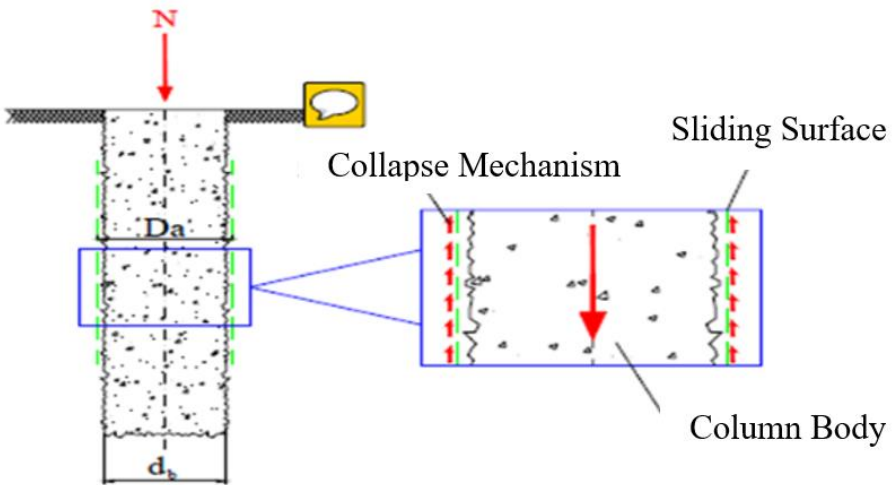

Figure 3. *Behaviour of the Jet grout column [10].*

Adhesion reduction factor in relation to the slip surface that may occur around the production perimeter of the Jet grouting column:

In cohesive, i.e. fine-grained soils;
$\alpha = 1$ for normally consolidated soils
$\alpha = 0.45$ in over consolidated soils
$K_s > 1$ in granular soils

The choice of column diameter is very important here. The average column diameter to be used in the design should be designed to be on the safe side of the diameter to be made in the field.

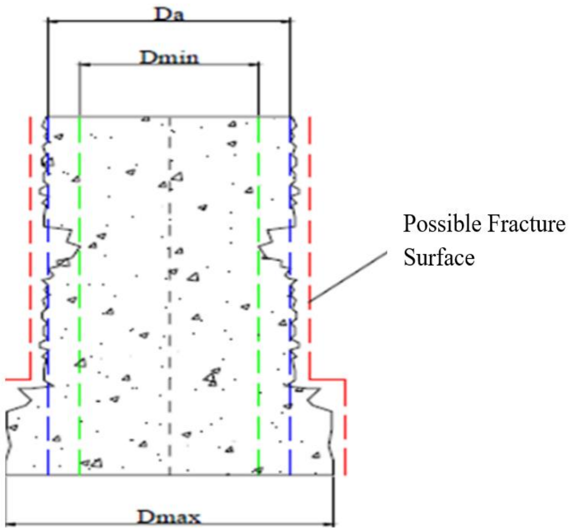

Figure 4. *Possible slip surface in the Jet grout column manufactured in the ground [10].*

Accurate determination of the column diameter and the adjustment of the reinforcement factor, either 0.45 or 1, are crucial when considering the effects that jet-grout columns experience during installation in granular soils, with soil pressure temperatures ranging from 1 to 1.4 [17].

Before theoretically assessing the bearing capacity of bored piles, it is also important to evaluate the potential negative environmental impacts associated with jet-grout columns. The strength of solidified clay can reach values as high as 4 MPa, while sandy gravels can achieve strengths of up to 12 MPa. For this analysis, a representative value of 6 MPa was selected.

The parameters of the jet grout columns demonstrate full mobility, typically resulting in minimal settlement. The amount of settlement required to achieve full mobilization of the end bearing capacity is also quite small [17]. Data presented in Tables 7 and 8 were compiled by Garassino.

Table 8. *Limit values used for column design in granular soils [17].*

Pile Type	Creep Force Reduction Factor		Limit Values for Unit Wall Friction	Tip Power reduction Factor
	δ/φ	**Ks**	**τ** (kPa)	ξ
Bored Pile	0,6	0,5-0,65	100-200	0,33-0,5
Drive Pile (Open End)	2/3	0,65-0,95	120	0,7-0,8
Drive Pile (Closed End)	0,75	1,0-1,5	120-180	1,0
Jet Grout Column	1	1,0-2	≥180	1,0

Table 9. *Limit values used for Jet grout column design in cohesive, i.e. fine-grained soils [17].*

Pile Type	Creep Force Reduction Factor		Limit Values for Unit Wall Friction	Tip Power reduction Factor
	α (Normal Consolidated)	**α (Over Consolidated)**	**τ** (kPa)	ξ
Bored Pile	0,9	0,35	275	0,66

Table 9 (cont). *Limit values used for Jet grout column design in cohesive, i.e. fine-grained soils [17].*

Drive Pile (Open End e: outside, i: inside)	0,95e 0,80i	0,40e 0,35i	200	0,7
Drive Pile (Closed End)	0,95	0,45	200	0,8
Jet Grout Column	1	0,45	280	1

C. GROUND IMPROVEMENT WITH COLUMNS FORMED IN THE GROUND

Soil consolidation refers to the process of altering the behavior of a soil mass through various production techniques [17]. The calculations for consolidation can be performed using two distinct methods: the first involves calculating the bearing capacity, while the second focuses on block analysis, which is based on limiting settlements.
The bearing capacity calculation technique is further divided into two components: group bearing capacity and block analysis. These methods help assess the overall performance and stability of the soil under applied loads.

C.1. Group Bearing Capacity Calculation of Load-Bearing Elements

The bearing capacity of the whole group is the sum of the bearing capacity of the Jet grouting columns within the group (Eq.18).

$$P_{ul(grup)} = \beta \; n \; m \; P_{ul(column)} \tag{18}$$

C.2. Block Analysis Method

The bearing capacity of the block considers the group of jet grouting columns as a cohesive unit. In this approach, the bearing capacity is determined by the friction force acting on the side surfaces and the bearing force on the bottom surface of the prism formed by the group (Eq. 19) (see Figure 5). This method allows for a comprehensive assessment of the group's performance under load.

$$P_{ul(grup)} = B.L.Q_b + 2(B+L).(h_2.Q_{12(ort)} - h_1.Q_{11(ort)}) \tag{19}$$

If there is no negative surface friction, h1 0 and h2 H should be accepted.

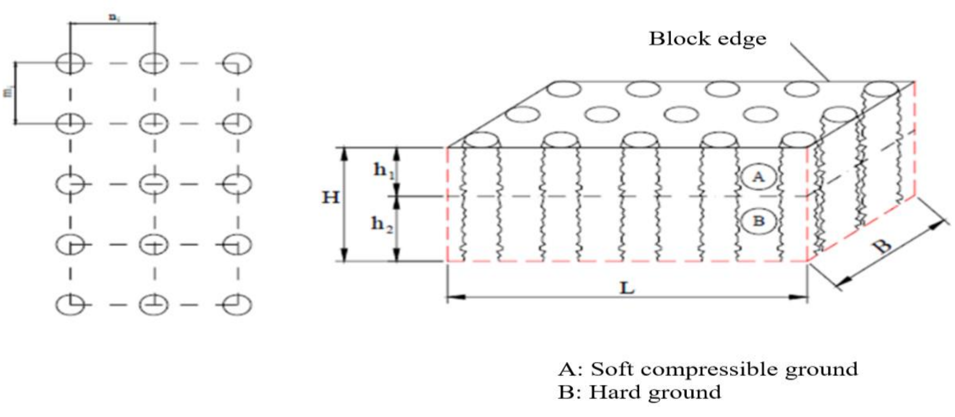

Figure 5. *Total/block bearing capacity of the soil improved with jet grout columns [17]*

III. CALCULATION METHOD

A. DETERMINATION OF MAXIMUM SHEAR MODULUS OF SOIL

The initial step in calculating columns with high shear strength achieved through the mixing of cement and soil is to determine the maximum shear modulus of the soil and to estimate the earthquake magnitudes.

To accomplish this, it is essential to establish the soil shear wave velocity profile. This can be done directly using methods such as Down-Hole or Suspension PS Logging, or indirectly through field test results, including SPT, CPT, and PMT. For this purpose, the shear wave velocity can be calculated using the following equation (Eq. 20) [18][19]:

$$V_s=62{,}14.\ N^{0{,}219}.\ H^{0{,}230}.\ F \tag{20}$$

The correction factor shall be 1.000 for clay soils, 1.091 for fine sands, 1.029 for medium grained sands, 1.073 for coarse grained sands, 1.151 for sand and gravel and 1.485 for gravelly soils.

B. UNIT AREA RATIO METHOD AND DETERMINATION OF SHEAR STRESSES

If the liquefaction analysis needs to be adjusted, guidelines for selecting methods that minimize liquefaction damage will initiate a process to determine the most suitable ground treatment for the site. In this context, Hayden and Baez outline the procedural steps for stone column applications.

The first step involves selecting an appropriate column diameter and spacing, followed by an iterative process for the columns composed of a soil mixture with a high shear modulus. The shear moduli of these columns will be defined based on the uniaxial cylindrical compressive test strengths (fJG) from columns located on sites with similar conditions, which may result from varying field application studies or initial contractor assessments. This information must be validated through practical experience during the construction phase.

Specimens obtained from the core samples of the jet grout columns will be subjected to uniaxial cylindrical tests, allowing for the calculation of the moduli of elasticity (E_{JG}) and shear (G_{JG}) based on a Poisson's ratio of 0.5 under the specified temperature conditions (see Eq. 21 - Eq. 25).

Elastic Shear Modulus (Eq.20):

$$E_{JG}=4730\sqrt{f_{JG}}\ \text{(MPa)} \tag{21}$$

Shear Modulus (Eq.21):

$$G_{JG}=\frac{E_{JG}}{2(1+v)} \tag{22}$$

Area Relocation Rate (Equation 22 and Equation 23):

$$ar=\frac{A_{JG}}{A} \tag{23}$$

$$as=\frac{A_S}{A}=1-ar \tag{24}$$

Shear Modulus of Shear Velocity (Eq.24):

$$G_s=\rho V_S{}^2 \tag{25}$$

In the later stages of the analysis, the fundamental principles of calculation rely on the distribution of shear stresses among the columns that are uniformly arranged over the earthquake-resistant unit area, as well as the interaction between these columns and the surrounding soil, determined by the ratio of their shear moduli.

It is recognized that in alluvial soils with potential for liquefaction, the shear wave velocity typically remains below 200 m/s. Consequently, the ratio of the shear modulus of the mixture produced from the jet grouting process to the soil's shear modulus is generally maintained between 15 and 160 times that of the columns. This ratio emphasizes the impact of the chosen application diameter and size range, leading to more pronounced effects on the performance of the columns. since the shear wave velocity will be low in soft soils, it will attract horizontal earthquake forces. The soil beneath the structure mentioned was strengthened and its strength increased with the jet grout method related with figure 6.

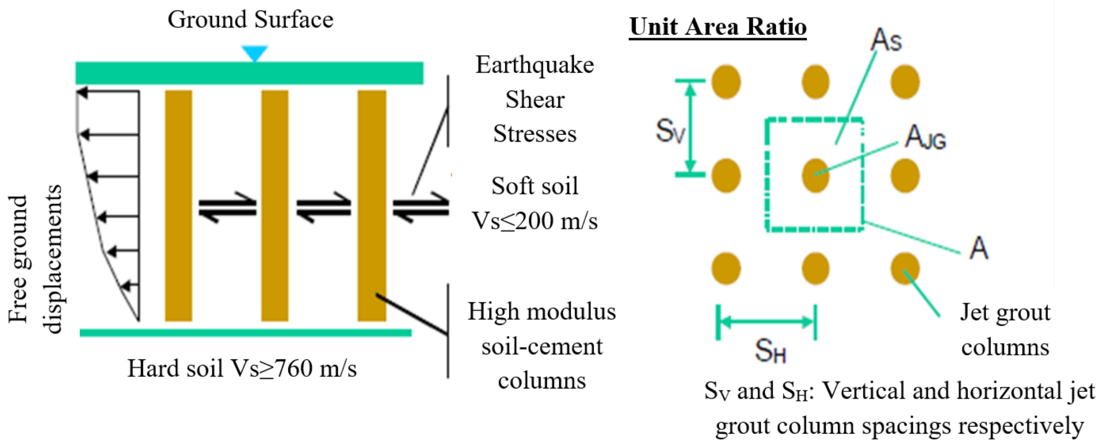

Figure 6. *Dispersion model of earthquake shear waves and definition of unit cell*

C. STRUCTURAL CONTROLS

To mitigate the risk of liquefaction in the ground between the columns, it is essential that the columns possess a high shear modulus and sufficient resistance to the shear forces acting upon them. To ensure the adequacy of the column cross-section against the shear force V_{JG}, the following equation (Eq. 26) is referenced. In this equation, the cement mix is evaluated under specific design conditions, with the reinforcing components of the columns treated as low-decay elements:

$$V_{JG}=0,3\sqrt{f_{JG}}\,A_{jG} \tag{26}$$

If similar results are found here with the help of similar results obtained by experience from previously obtained data, they should be applied to a safety coefficient value of 2 under minimum conditions (f_{JG}). The results should be checked with in-situ core equivalent samples carried out during the production phase.

D. FINDING

D. 1. Field Findings

For the foundation excavation of 3.70m and foundation depth of 3.20m, the soil safety stress was 0.81kg/cm² and the soil bearing capacity was 2.43 kg/cm². According to the drilling data, the vertical bedding coefficient was calculated as 750-1250ton/m³ and it was recommended to be taken between these values. The groundwater level was measured at 4 m and it was stated that it may change up and down by 1m depending on the seasons. It is recommended to take a structure importance coefficient of 1.4. There is no potential risk of liquefaction.

Geotechnical parameters (unit volume weights, cohesion, internal friction angle and volumetric compression coefficients, fine grain ratio) according to the laboratory data obtained from 3 12.50 m (sk1-sk2-sk3) borings in the field; for SK1 (3.50-4.0m); 18.74 KN/m³, cohesion 30.96 kN/m², internal friction angle 2o and volumetric compaction coefficient 0.0475cm²/kgf, for SK2 (2.50-3.0m); unit volume weight 18.45Kn/m³, cohesion 34. 40 kN/m², internal friction angle 3o and M_v=0,0338cm²/kgf, for SK3 (3.0-3.50m); 18.14Kn/m³, c=42.99 kN/m², internal friction angle 3o and volumetric compaction coefficient 0,0286 cm²/kgf. As a result of the sieve analysis, the average percentage (%) of those passing through the sieve numbered 200 was 95 and the SPT (N) averages were reduced by 1/2 and taken as 26.

According to the average of the geophysical data, the average thickness of the 1st layer is 4.25m, and since the excavation depth was determined as 3.70m, the 2nd layer data (after 4.25m) were taken into consideration. Accordingly, the average shear wave velocity for the 2nd layer is 315m/sec, the average Poisson's ratio is 0.45, the average modulus of elasticity is 552200 kN/m², and the average ground dominant vibration period is 0.68 sec.

D. 2. Bearing Capacity of Jet grout Column Group

P_{ugrup} was calculated as 78172.878 kN, large foundation as +8685.875 kN and small foundation as 86858.753 kN. In addition, the bearing capacity values obtained for large foundations and small foundations are given below (Table 9).

Table 10. *Bearing capacity values obtained for foundations*

No	A_c (m²)	σ_{vo} (kN/m²)	σ'_{VO} (kN/m²)	N_q	K_O	q_b (kN/m²)	P_{base} (kN)	P_{lat} (kN)	P_u (kN)	σ_{Ult} (kN/m²)
1	0,503	5,499	5,499	1,122	0,948	288	144,76	10,857	155,622	89,024
1	0,503	219,96	114,66	1,122	0,948	288	144,76	423,436	568,201	135,421

D. 3. Soil Liquefaction Values

According to the data obtained from the ground improvement site, liquefaction analysis results were performed before ground improvement and no liquefaction was observed at the end of the calculation (Table 10).

Table 11. *Soil Liquefaction Values*

No	z	σ_{vo} (kN/m²)	σ'_{VO} (kN/m²)	SPN	C_n	N60	α	β	$N_{1,60}$	C_m	CSR 7,5	τ (kPa)	r_d	τ_{av}	FS	Result
1	0,3	5,499	5,499	26	1,7	45	5	1,2	33	1,11	0,238	1,45	0,998	0,591	2,46	Sufficient
2	12	219,96	114,66	26	0,913	27	5	1,2	18	1,11	0,386	43,055	0,854	20,21	2,13	Sufficient

IV. CONCLUSION

The site investigation study has been prepared for the planned construction of a 1,000 m² building with a basement, ground floor, and three additional stories by the Düzce Provincial Directorate of the Ministry of Family and Social Policies on a 1,918.84 m² parcel (No. 535) in the Kiremitocağı Neighborhood, Central District, Treasury of Finance. According to this study, the area is situated in a

1st degree earthquake zone. The revised zoning plan approved on March 11, 2005, designates this site as within Precautionary Area 2 (PA-2), where construction is prohibited without appropriate measures.

Although the liquefaction analysis indicates that there is no risk of liquefaction, improvement of the site is necessary due to its location within the North Anatolian Fault zone system. For the existing building load of 7,606 tons, with a foundation excavation depth of 3.70 m and a foundation depth of 3.20 m, the soil safety stress is determined to be 0.81 kg/cm², while the soil bearing capacity is assessed at 2.43 kg/cm². Drilling data suggest a vertical bedding coefficient of 750-1,250 t/m³, and it is recommended that this value be adopted within that range. The groundwater level in the area is measured at 4 m, with potential seasonal fluctuations of ±1 m.

For the large foundations, with a long side of 36.78 m and a short side of 26.79 m, the foundation excavation is 3.70 m. The nearest column is located 0.5 m from the foundation corner, with 12 columns in the x-direction and 9 columns in the y-direction. The columns will extend to a length of 12 m and have a diameter of 0.8 m, with spacing between columns of 3.18 m and 2.94 m. The groundwater level after foundation excavation is anticipated to be 0.3 m.

The small foundations consist of 108 columns, with a long side of 16.8 m and a short side of 4.8 m, also featuring a foundation excavation of 3.70 m. The distance from the nearest column to the foundation corner is again 0.5 m, with 6 columns in the x-direction and 2 in the y-direction. These columns will also be 12 m long with a diameter of 0.8 m and spaced 3.00 m apart. The groundwater level after foundation excavation for these foundations is also projected to be 0.3 m. In total, there will be 120 columns, including both large and small foundations.

Based on the data, soil improvement was executed using the jet grouting method, yielding the following results: the safety stress of the improved ground is 1.33 kg/cm², the improved vertical soil bearing coefficient (k_0) is 1,596 t/m³, and the load-bearing capacity of the jet grout column group is 86,858.753 kN. The expected settlement following the improvement is 0.22 mm. The ground classification after improvement is designated as "C," and the local soil class is classified as "Z4," indicating that the improvements have been considered as appropriate.

Finally, since the shear wave velocity will be low in soft soils, it will attract horizontal earthquake forces. The soil beneath the structure mentioned was strengthened and its strength increased with the jet grout method and mentioned in above.

ACKNOWLEDGEMENTS: We thank the Düzce Provincial Directorate of Environment and Urbanization for their contributions to the work.

V. REFERENCES

[1] Z. F. Wang, S. L. Shen, and W. C. Cheng, "Lateral Displacement Induced by Jet Grouting in Clayey Soils," *Géotechnique*, vol. 67, no. 7, pp. 621–630, 2017.

[2] S. L. Shen, Z. F. Wang, and W. C. Cheng, "Estimation of Liquefaction Prevention Using Jet Grouting," *Geotechnical Engineering*, vol. 67, no. 7, pp. 621–630, 2017.

[3] H. Yalçın, Z. Kaya, C. C. Çadır, E. Uncuoğlu, A. Erol, and M. Akın, "Improvement of an Undisturbed Peat Soil with Jet Grout Columns: Physical and Numerical Modeling," *Arabian Journal for Science and Engineering*, vol. 48, no. 1, pp. 105–115, 2023.

[4] R. K. N. Wong, Yee Foo Weng, Gan Kok Leong and Shih-Hao Cheng "A Case Study of Effectiveness of Large Diameter Jet Grout for Soil Improvement Works in Soft Marine Clay," in *Geotechnics for Sustainable Infrastructure Development*, Springer vol. 62, no. 1, pp. 649–655, 2019.

[5] H. Güllü, "Prediction of Rheological Characteristics of Jet Grout Mixtures Using Genetic Programming," *Neural Computing and Applications*, vol. 29, no. 1, pp. 251-260, 2017.

[6] G. Mısır, "Jet Grout Yöntemi İle Zemin İyileştirme ve Deplasman Tahmini: Vaka Analizi," *Avrupa Bilim ve Teknoloji Dergisi*, c. 18, ss. 290-299, 2020.

[7] M. J. Lenard, P. Alam, and G. R. Madey, "The Application of Neural Networks and a Qualitative Response Model to the Auditor's Going Concern Uncertainty Decision," *Decision Science*, vol. 26, no. 2, pp. 209–227, 1995.

[8] M. N. Vu and Q. H. Le, "Large Soil-Cement Columns in Vietnam," in *Geotechnics for Sustainable Infrastructure Development*, Springer, vol. 62, no. 1, pp. 555–562, 2019.

[9] A. Ateş, "Yozgat (Şefaatli) İlçesi Adalet Sarayı Temel Zemininin Sıvılaşma Potansiyelinin Araştırılması ve Zemin İyileştirilmesi: Vaka Analizi," *Düzce Üniversitesi Bilim ve Teknoloji Dergisi*, c. 5, ss. 258-272, 2017.

[10] H. B. Seed and I. M. Idriss, "Title of the Paper," *Journal of Soil Mechanics & Foundations Div.*, vol. 97, no. 9, pp. 1249-1273, 1971.

[11] S. S. C. Liao and R. V. Whitman, "Overburden Correction Factors for SPT in Sand," *Journal of Geotechnical Engineering*, ASCE, vol. 112, no. 3, pp. 373-377, 1986.

[12] M. R. K., "Application of Linear Statistical Model of Earthquake Magnitude Versus Fault Length in Estimating Maximum Expectable Earthquakes," *Geology*, vol. 5, pp. 464-466, 1977.

[13] D. L. Wells and K. J. Coppersmith, "New Empirical Relationships Among Magnitude, Rupture Length, Rupture Width, Rupture Area, and Surface Displacement," Bull. Seismol. Soc. Am., vol. 84, pp. 974-1002, 1994.

[14] R. Ulusay, E. Tuncay, H. Sonmez, and C. Gokceoglu, "An Attenuation Relationship Based on Turkish Strong Motion Data and Iso-acceleration Map of Turkey," *Engineering Geology*, vol. 74, pp. 265-291, 2004.

[15] T. L. Youd et al., "Liquefaction Resistance of Soils: Summary Report from the 1996 NCEER and 1998 NCEER/NSF Workshops on Evaluation of Liquefaction Resistance of Soils," *Journal of Geotechnical and Geoenvironmental Engineering*, vol. 127, no. 10, pp. 817-833, 2001.

[16] A. W. Skempton, "Standard Penetration Test Procedures and the Effects in Sands of Overburden Pressure, Relative Density, Particle Size, Aging, and Overconsolidation," *Geotechnique*, vol. 36, no. 3, pp. 425-447, 1986.

[17] L. A. Grassino, "Design Procedures for Jet-Grouting," *in Seminar on Jet Grouting*, Singapore, Apr. 7, 1997.

[18] Y. Ohta and N. Goto, "Empirical Shear Wave Velocity Equations in Terms of Characteristic Soil Indexes," *Earthquake Engineering & Structural Dynamics*, vol. 6, no. 2, pp. 167-187, 1978.

[19] A. Özyanki, H. Dindar, and A. Ekinci, "Killi Zeminlerde Çok Kanallı Yüzey Dalgası Analizi Yöntemi ile Elde Edilen Kayma Dalga Hızı ile Plastisite İndisi ve Standart Penetrasyon Sayısı Korelasyonu," *Avrupa Bilim ve Teknoloji Dergisi*, c. 20, ss. 490-497, 2020.

[20] *İnşaat Mühendisliğinde Zeminlerin Sınıflandırılması,* Türk Standartları Enstitüsü TS 1500, 2000.